and solid tumor are good targets for cytotoxic CD4+ T cells.

The present study clearly demonstrated that $WT1_{332}$ TCR-transduced CD4+ T cells displayed helper activity for WT1-specific CTL induction and cytotoxicity against leukemia cells. This observation that $WT1_{332}$ TCR-transduced CD4+ T cells had 2 function (helper and cytotoxicity) raised a hypothesis that function of CD4+ T cells was divided into 2 phases: helper and cytotoxicity phases. It is generally known that IL-2 derived from CD4+ T cells is a crucial factor for exhibition of helper activity to enhance CTL function and that undifferentiated, proliferative CD4+ T cells can more produce IL-2 compared to differentiated, nonproliferative CD4+ T cells. $WT1_{332}$ TCR-transduced CD4+ T cells rapidly proliferated and produced a large amount of IL-2 at early phase within 1 month from the beginning of the culture, but stopped producing IL-2 with less proliferation at late phase after repeated antigen-stimulation (data not shown). It was previously reported that cytotoxic CD4+ T cells appeared after repeated antigen-stimulation and possessed a phenotype-like terminally differentiated effector cells such as $CD27^-$, $CD28^-$, and $CD57^+$.[41] These findings supported our hypothesis that CD4+ T cell might transiently exert a helper activity (helper CD4+ T cells) at early phase and then a cytotoxic activity (cytotoxic CD4+ T cells) at late phase.

As WT1 was selected from 75 defined tumor antigens to rank as the most promising cancer vaccine target in a prioritization study carried out by National Cancer Institute,[13] WT1-targeted cancer immunotherapy is thought to be also the most promising strategy for cure of cancer. TCR gene therapy using $WT1_{332}$-specific TCR should be a useful tool for cancer immunotherapy because the TCR-transduced CD4+ T cells elicited both a helper activity for the induction of WT1-specific CD8+ CTLs and a cytotoxic activity against tumor. Furthermore, combination TCR gene therapy of HLA class I-restricted, WT1-specific TCR and HLA class II-restricted, $WT1_{332}$-specific TCR is expected to be more efficient. In addition, $WT1_{332}$-specific TCR gene therapy should be also effective in combination with HLA class I-restricted WT1 peptide vaccine.

CONFLICTS OF INTEREST/ FINANCIAL DISCLOSURES

Supported, in part, by a Grant-in-Aid for Young Scientists (WAKATE B-22700896) from the Ministry of Education, Science, Sports, Culture, and Technology and the Ministry of Health, Labor and Welfare of Japan.

All authors have declared there are no financial conflicts of interest in regards to this work.

REFERENCES

1. Hohenstein P, Hastie ND. The many facets of the Wilms' tumour gene, WT1. *Hum Mol Genet.* 2006;15:R196–R201.
2. Yamagami T, Sugiyama H, Inoue K, et al. Growth inhibition of human leukemic cells by WT1 (Wilms tumor gene) antisense oligodeoxynucleotides: implications for the involvement of WT1 in leukemogenesis. *Blood.* 1996;87:2878–2884.
3. Inoue K, Tamaki H, Ogawa H, et al. Wilms' tumor gene (WT1) competes with differentiation-inducing signal in hematopoietic progenitor cells. *Blood.* 1998;91:2969–2976.
4. Tsuboi A, Oka Y, Ogawa H, et al. Constitutive expression of the Wilms' tumor gene WT1 inhibits the differentiation of myeloid progenitor cells but promotes their proliferation in response to granulocyte-colony stimulating factor (G-CSF). *Leuk Res.* 1999;23:499–505.
5. Call KM, Glaser T, Ito CY, et al. Isolation and characterization of a zinc finger polypeptide gene at the human chromosome 11 Wilms' tumor locus. *Cell.* 1990;60:509–520.
6. Gessler M, Poustka A, Cavenee W, et al. Homozygous deletion in Wilms tumours of a zinc-finger gene identified by chromosome jumping. *Nature.* 1990;343:774–778.
7. Sugiyama H. WT1 (Wilms' tumor gene 1): biology and cancer immunotherapy. *Jpn J Clin Oncol.* 2010;40:377–387.
8. Oka Y, Elisseeva OA, Tsuboi A, et al. Human cytotoxic T-lymphocyte responses specific for peptides of the wild-type Wilms' tumor gene (WT1) product. *Immunogenetics.* 2000;51:99–107.
9. Ohminami H, Yasukawa M, Fujita S. HLA class I-restricted lysis of leukemia cells by a CD8(+) cytotoxic T-lymphocyte clone specific for WT1 peptide. *Blood.* 2000;95:286–293.
10. Oka Y, Tsuboi A, Taguchi T, et al. Induction of WT1 (Wilms' tumor gene)-specific cytotoxic T lymphocytes by WT1 peptide vaccine and the resultant cancer regression. *Proc Natl Acad Sci USA.* 2004;101:13885–13890.
11. Tsuboi A, Oka Y, Kyo T, et al. Long-term WT1 peptide vaccination for patients with acute myeloid leukemia with minimal residual disease. *Leukemia.* 2011;26:1410–1413.
12. Morita S, Oka Y, Tsuboi A, et al. A phase I/II trial of a WT1 (Wilms' tumor gene) peptide vaccine in patients with solid malignancy: safety assessment based on the phase I data. *Jpn J Clin Oncol.* 2006;36:231–236.
13. Cheever MA, Allison JP, Ferris AS, et al. The prioritization of cancer antigens: a national cancer institute pilot project for the acceleration of translational research. *Clin Cancer Res.* 2009;15:5323–5337.
14. Ochi T, Fujiwara H, Okamoto S, et al. Novel adoptive T-cell immunotherapy using a WT1-specific TCR vector encoding silencers for endogenous TCRs shows marked antileukemia reactivity and safety. *Blood.* 2011;118:1495–1503.
15. Xue SA, Gao L, Hart D, et al. Elimination of human leukemia cells in NOD/SCID mice by WT1-TCR gene-transduced human T cells. *Blood.* 2005;106:3062–3067.
16. Parkhurst MR, Yang JC, Langan RC, et al. T cells targeting carcinoembryonic antigen can mediate regression of metastatic colorectal cancer but induce severe transient colitis. *Mol Ther.* 2011;19:620–626.
17. Davis JL, Theoret MR, Zheng Z, et al. Development of human anti-murine T-cell receptor antibodies in both responding and nonresponding patients enrolled in TCR gene therapy trials. *Clin Cancer Res.* 2010;16:5852–5861.
18. Marshall NB, Swain SL. Cytotoxic CD4 T cells in antiviral immunity. *J Biomed Biotechnol.* 2011;2011:954602.
19. Janssen EM, Lemmens EE, Wolfe T, et al. CD4 + T cells are required for secondary expansion and memory in CD8 + T lymphocytes. *Nature.* 2003;421:852–856.
20. Hunder NN, Wallen H, Cao J, et al. Treatment of metastatic melanoma with autologous CD4 + T cells against NY-ESO-1. *N Engl J Med.* 2008;358:2698–2703.
21. Quezada SA, Simpson TR, Peggs KS, et al. Tumor-reactive CD4(+) T cells develop cytotoxic activity and eradicate large established melanoma after transfer into lymphopenic hosts. *J Exp Med.* 2010;207:637–650.
22. Fujiki F, Oka Y, Tsuboi A, et al. Identification and characterization of a WT1 (Wilms Tumor Gene) protein-derived HLA-DRB1*0405-restricted 16-mer helper peptide that promotes the induction and activation of WT1-specific cytotoxic T lymphocytes. *J Immunother.* 2007;30:282–293.
23. Fujiki F, Oka Y, Kawakatsu M, et al. A WT1 protein-derived, naturally processed 16-mer peptide, WT1(332), is a promiscuous helper peptide for induction of WT1-specific Th1-type CD4(+) T cells. *Microbiol Immunol.* 2008;52:591–600.
24. Guo Y, Niiya H, Azuma T, et al. Direct recognition and lysis of leukemia cells by WT1-specific CD4 + T lymphocytes in an HLA class II-restricted manner. *Blood.* 2005;106:1415–1418.

25. Fujiki F, Oka Y, Kawakatsu M, et al. A clear correlation between WT1-specific Th response and clinical response in WT1 CTL epitope vaccination. *Anticancer Res.* 2010;30:2247–2254.
26. ZumLa A, Marguerie C, So A, et al. Co-expression of human T cell receptor chains with mouse CD3 on the cell surface of a mouse T cell hybridoma. *J Immunol Methods.* 1992;149:69–76.
27. Furukawa T, Koike T, Ying W, et al. Establishment of a new cell line with the characteristics of a multipotential progenitor from a patient with chronic myelogenous leukemia in early erythroblastic crisis. *Leukemia.* 1994;8:171–180.
28. Elisseeva OA, Oka Y, Tsuboi A, et al. Humoral immune responses against Wilms tumor gene WT1 product in patients with hematopoietic malignancies. *Blood.* 2002;99:3272–3279.
29. Oji Y, Kitamura Y, Kamino E, et al. WT1 IgG antibody for early detection of nonsmall cell lung cancer and as its prognostic factor. *Int J Cancer.* 2009;125:381–387.
30. Hayashida M, Kawano H, Nakano T, et al. Cell death induction by CTL: perforin/granzyme B system dominantly acts for cell death induction in human hepatocellular carcinoma cells. *Proc Soc Exp Biol Med.* 2000;225:143–150.
31. Chattopadhyay PK, Yu J, Roederer M. A live-cell assay to detect antigen-specific CD4 + T cells with diverse cytokine profiles. *Nat Med.* 2005;11:1113–1117.
32. Frankel TL, Burns WR, Peng PD, et al. Both CD4 and CD8 T cells mediate equally effective *in vivo* tumor treatment when engineered with a highly avid TCR targeting tyrosinase. *J Immunol.* 2010;184:5988–5998.
33. Tsuji T, Yasukawa M, Matsuzaki J, et al. Generation of tumor-specific, HLA class I-restricted human Th1 and Tc1 cells by cell engineering with tumor peptide-specific T-cell receptor genes. *Blood.* 2005;106:470–476.
34. Ray S, Chhabra A, Chakraborty NG, et al. MHC-I-restricted melanoma antigen specific TCR-engineered human CD4 + T cells exhibit multifunctional effector and helper responses, *in vitro*. *Clin Immunol.* 2010;136:338–347.
35. Ha SP, Klemen ND, Kinnebrew GH, et al. Transplantation of mouse HSCs genetically modified to express a CD4-restricted TCR results in long-term immunity that destroys tumors and initiates spontaneous autoimmunity. *J Clin Invest.* 2010;120:4273–4288.
36. Zhao Y, Zheng Z, Khong HT, et al. Transduction of an HLA-DP4-restricted NY-ESO-1-specific TCR into primary human CD4 + lymphocytes. *J Immunother.* 2006;29:398–406.
37. Scholten KB, Turksma AW, Ruizendaal JJ, et al. Generating HPV specific T helper cells for the treatment of HPV induced malignancies using TCR gene transfer. *J Transl Med.* 2011;9:147.
38. Ossendorp F, Mengedé E, Camps M, et al. Specific T helper cell requirement for optimal induction of cytotoxic T lymphocytes against major histocompatibility complex class II negative tumors. *J Exp Med.* 1998;187:693–702.
39. Wilkinson TM, Li CK, Chui CS, et al. Preexisting influenza-specific CD4 + T cells correlate with disease protection against influenza challenge in humans. *Nat Med.* 2012;18:274–280.
40. Hidalgo LG, Einecke G, Allanach K, et al. The transcriptome of human cytotoxic T cells: similarities and disparities among allostimulated CD4(+) CTL, CD8(+) CTL and NK cells. *Am J Transplant.* 2008;8:627–636.
41. Brown DM. Cytolytic CD4 cells: Direct mediators in infectious disease and malignancy. *Cell Immunol.* 2010;262:89–95.
42. Matsushita N, Ghazizadeh M, Konishi H, et al. Association of ovarian tumor epithelium coexpressing HLA-DR and CA-125 antigens with tumor infiltrating cytotoxic T lymphocytes. *J Nihon Med Sch.* 2003;70:40–44.
43. Altomonte M, Fonsatti E, Visintin A, et al. Targeted therapy of solid malignancies via HLA class II antigens: a new biotherapeutic approach? *Oncogene.* 2003;22:6564–6569.
44. Rimsza LM, Roberts RA, Miller TP, et al. Loss of MHC class II gene and protein expression in diffuse large B-cell lymphoma is related to decreased tumor immunosurveillance and poor patient survival regardless of other prognostic factors: a follow-up study from the Leukemia and Lymphoma Molecular Profiling Project. *Blood.* 2004;103:4251–4258.
45. Stevanović S, Griffioen M, Nijmeijer BA, et al. Human allo-reactive CD4 + T cells as strong mediators of anti-tumor immunity in NOD/scid mice engrafted with human acute lymphoblastic leukemia. *Leukemia.* 2012;26:312–322.
46. Løvig T, Andersen SN, Thorstensen L, et al. Strong HLA-DR expression in microsatellite stable carcinomas of the large bowel is associated with good prognosis. *Br J Cancer.* 2002;87:756–762.
47. Bernsen MR, Håkansson L, Gustafsson B, et al. On the biological relevance of MHC class II and B7 expression by tumour cells in melanoma metastases. *Br J Cancer.* 2003;88:424–431.
48. Friedman KM, Prieto PA, Devillier LE, et al. Tumor-specific CD4 + melanoma tumor-infiltrating lymphocytes. *J Immunother.* 2012;35:400–408.

pISSN 1598-2998, eISSN 2005-9256

Cancer Res Treat. 2013;45(3):155-161 http://dx.doi.org/10.4143/crt.2013.45.3.155

Review Article Open Access

Stereotactic Body Radiotherapy for Early Stage Lung Cancer

Yasushi Nagata, MD, PhD

Department of Radiation Oncology, Hiroshima University, Hiroshima, Japan

Stereotactic body radiation therapy (SBRT) is a newly developed technique currently in clinical use. SBRT originated from stereotactic radiosurgery for intracranial tumors. SBRT has been widely used clinically for lung cancer. The practice of SBRT demands different kinds of patient fixation, breathing control, target determination, treatment planning, and verifications. The history and current standard technique are reviewed. Clinical studies of lung cancer showed high local control rates with acceptable toxicities. Past and on-going clinical trials are reviewed.

Key words
Radiosurgery, Early stage lung cancer, Stereotactic body radiation therapy, Stereotactic ablative radiotherapy, Stereotactic radiotherapy, Lung neoplasms, Conformal radiotherapy

Correspondence: Yasushi Nagata, MD, PhD
Department of Radiation Oncology, Hiroshima University, Hiroshima 734-8551, Japan
Tel: 81-82-257-1545
Fax: 81-82-257-1546
E-mail: nagat@hiroshima-u.ac.jp
Received June 14, 2013
Accepted June 20, 2013

Introduction

Stereotactic radiotherapy (SRT) is method to deliver highly precise radiation to intracranial tumors that can maintain fixed precision within 1-2 mm. This treatment method aims to minimize the radiation dose administered to normal tissues and increase the radiation administered to the tumor by accurately focusing radiation onto the target lesion (hereafter "target"). SRT was originally developed for clinical application in the 1960s as "gamma knife radiosurgery," most commonly employing single high dose radiation, and evolved to the current form after linear accelerator (LINAC)-based radiosurgery was introduced by 1983. Both techniques initially were developed for treating intracranial brain tumors. The application of the stereotactic technique on the trunk of the body was initiated in the 1990s. In the USA, this is known as stereotactic body radiation therapy (SBRT) or stereotactic ablative external radiotherapy, while in Europe, it is known as extracranial stereotactic radiotherapy. In Japan

it is commonly known as pin-pointed radiotherapy. Its first recognized use was by Blomgren et al. [1] of the Karolinska Institute in 1991, while in Japan, it was implemented by Uematsu et al. [2] in 1994. However, the main problem with performing SBRT on tumors of the trunk as opposed to brain tumors was tumor movement caused by bodily and respiratory movements. Therefore, when performing SBRT for tumors of the body trunk, it is extremely important to establish accurate patient fixation, breathing control systems, and verification of the irradiation field prior to each treatment.

Practice of SBRT

1. Patient fixation

To restrain the bodies of patients during treatment, it is important to have suitable fixation methods. Various vacuum contact-type braces are currently available for use in SBRT that involve styrofoam in a plastic body frame.

2. Breathing control

In lung tumors, tumor movement during respiration cannot be ignored. Methods that deal with the respiratory movement of patients can be broadly divided into the breath holding technique, the restricted respiration technique (abdominal compression), and respiratory gating technique. Efforts to reduce tumor movement during respiration (internal margin) are required.

The breath holding technique is a voice or light-gated intermittent irradiation system in which the patient temporarily suspends his/her breathing following an audible or light signal, allowing for irradiation. In this technique, breath is generally held at the resting expiratory level, and theoretically internal tumor volume, a radiation volume including tumor motion, is minimized, making it possible to set the minimal irradiated volume. In addition, devices can be used to help suspend breathing [3].

An alternative to this is the restricted respiration technique in which major movements of the patient's diaphragm are restricted by compressing the upper abdomen using either a belt or plate-like brace. Tumor movement is ascertained by fluoroscopy, and if found to be greater than 8-10 mm, it is common to restrict movement [4]. In practice, restriction of respiration is required owing to tumor movement greater than 8-10 mm in less than 25% of all patients.

In contrast to these methods, a respiratory gating technique has been developed that synchronizes irradiation with the respiratory phase (mainly the expiratory phase) while the patient breathes freely but periodically. This is a frequently used technique in which sensors are attached to the thoracic wall of the patient, or gold markers are introduced into the tumor [5], and irradiation is performed while sensing the patient's breathing.

3. Target determination and computed tomography (CT) imaging

In highly accurate treatment planning, using CT images usually taken at 1-3-mm intervals, radiation oncologists delineate the contour of the tumor and the organs at risk. The breath synchronization and breath holding methods mentioned above are a prerequisite of treatment, and CT images are obtained in accordance with these techniques. When the restricted respiration technique is employed, a prolonged or slow scan CT imaging technique is used in which images are obtained slowly, with a scan time of >4 seconds taken per slice to improve the accuracy of irradiation. It is important to be aware that the target definition differs according to these CT imaging techniques.

In recent years, 4-dimensional (4D) CT imaging technology has emerged, which involves placing infrared markers on the body surface of the patient to obtain a respiratory signal. Using this technique, target information (such as maximum intensity projection image) for the entire respiratory phase can be obtained. It is extremely useful in SBRT.

4. Treatment planning

Once the target is delineated using reconstructed 3-dimensional (3D) images such as Beam's eye view or Room's eye view, the radiation field is determined by combining various factors, including the direction and energy of radiation. Non-coplanar 3D conformal multiport irradiation and static multiple arc radiotherapy are often used. In these methods, using either fixed multiport irradiation with >6 ports or rotatory irradiation of >400°, an approximate equivalent dose distribution can be achieved. Target dose in treatment planning include homogeneous radiation dose within the target (within 10%) and reduction (<15%) of lung capacity (V20) of >20 Gy of radiation. It is possible to achieve this by administering 3D irradiation from a total of 6-8 fields, including irradiation at an angle of +/- 20-40° non-coplanar beams as well as coplanar beams to the body's axis (Fig. 1). Calculating the correct 3D radiation dose allowing for inhomogeneity correction is essential, as is the correction of the radiation dose due to the frame. Furthermore, attention should be paid to the radiation dose prescription used. In Japan, the isocenter is most often the radiation dose prescrip-

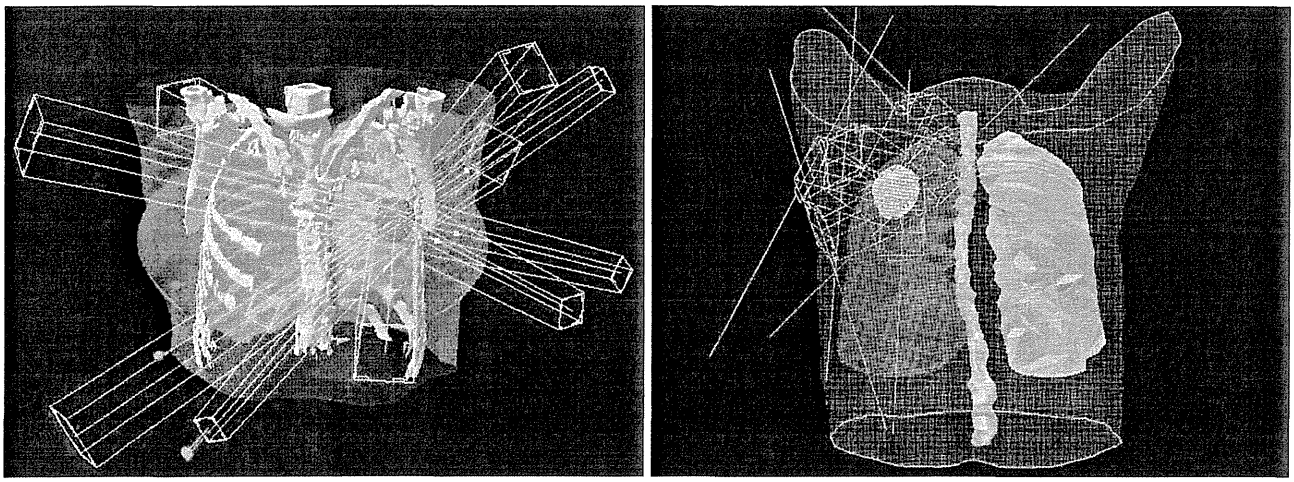

Fig. 1. A case of stereotactic body radiation therapy (SBRT) for early stage lung cancer (T1N0M0). SBRT is conducted on the left lung cancer by focusing radiation from six directions. Axial view, 3D image of radiation dose distribution.

tion point, while in Europe and the USA, the marginal dose of radiation at 80-90% is often used. It is important to note that treatment planning may differ according to the radiation field margin and the dose calculation method.

5. Pretreatment verification methods

Prior to each dose of irradiation, verification images are created and checked using a high-energy X-ray image, portal image, or in-room CT to confirm that the correct site is being irradiated. In SBRT in particular, it is essential to conduct verification prior to irradiation. To verify the reproducibility of irradiation before each treatment, verification images (confirmation images taken before irradiation using the imaging equipment) are obtained. Reproducibility of the body position with the simulation film during treatment planning is confirmed. As a result, administering irradiation within the usual error range of 2-3 mm is possible through verification of each result before each treatment. In the Japan Clinical Oncology Group (JCOG) 0403 multicenter collaborative clinical trial, a margin of 5 mm is essential. There are an increasing number of facilities that conduct pretreatment verification using either X-ray equipment attached to image-guided radiation therapy (IGRT) or by CT, with equipment set up in the same room as the radiotherapy equipment.

Clinical Results and Toxicities

1. Exposure dose and treatment outcomes

Many different fractionated irradiation techniques have been used: 12 Gy×4 fractions per radiation treatment [6], 10-12 Gy×5-6 fractions per radiation treatment [5], 7.5 Gy×8 fractions per radiation treatment [7], and 15 Gy×3 fractions per radiation treatment. Regardless of the technique used,

Table 1. Results of various clinical trials of stereotactic body radiation therapy for lung cancer

Reference	Total dose (Gy)	Daily dose (Gy)	Reference point	Local control n (%)	Median follow-up (mo)
Uematsu et al. (2001) [5]	50-60	10	80% Margin	47/50 (94)	36
Arimoto et al. (1998) [8]	60	7.5	Isocenter	22/24 (92)	24
Timmerman et al. (2010) [9]	54	18	80% Margin	54/55 (98)	34
Onimaru et al. (2003) [7]	48-60	6-7.5	Isocenter	20/25 (80)	17
Wulf et al. (2004) [10]	45-56.2	15-15.4	80% Margin	19/20 (95)	10
Nagata et al. (2005) [6]	48	12	Isocenter	44/45 (97)	30
Xia et al. (2006) [11]	70 (50)	7 (5)	Isocenter	41/43 (95)	27
Baumann et al. (2009) [12]	45	15	67% Margin	53/57 (92)	35

when the biological effective dose (BED) is >100 Gy, the local control rate is 88-96% with some variation (Table 1) [5-12]. In these different fractionated irradiation methods, the radiation dose, total dose, and number of fractionations are often extrapolated using a linear quadratic (LQ) model calculation based on α/β values. For example, when the α/β value of the tumor is 10, a radiation dose of 12 Gy×4 fractions corresponds to 88 Gy×2 fractions. Using SBRT technology, it is possible to substantially increase the radiation dose.

Fowler [13] demonstrated that the LQ model can be clinically applied with few fractionations and that good localized control can be achieved with a BED > 100 Gy. In addition, it is unclear whether the number of radiations in SBRT can ultimately be reduced to one. However, for radiobiological reasons, fractionated irradiation is advantageous as long as hypoxic fractions exist in the tumor. Results from the USA and Europe estimate that 3-5 fractionated irradiations are the minimum number of irradiations while single irradiation is unsatisfactory.

Onishi et al. [14] examined cases from 13 medical facilities throughout Japan and reported treatment outcomes. While the local control rate was 86%, in cases able to undergo irradiation of BED > 100 Gy with surgery, the 5-year survival rate was excellent with 90% for the IA stage and 84% for the IB stage [14].

In Europe and the USA, Wulf et al. [10], Timmerman et al. [9], Xia et al. [11], and Baumann et al. [12] all report favorable local effects. However, the number of cases in these papers, when compared to cases in Japan, may have had poorer prognosis because more unfavorable cases were treated as subjects.

2. Normal tissue toxicities

In clinical results, the risk of radiation pneumonitis with symptoms greater than Common Terminology Criteria for Adverse Events (CTCAE)—grade 3 is extremely low compared with conventional radiotherapy for stage III lung cancer. In other words, provided an isolated tumor of <4-5 cm in diameter is targeted in a lung, the irradiated volume of normal lung is within the permissible range. The majority of stage I lung cancer cases present asymptomatically, and care must therefore be taken with regard to treatment of emergent complications. However, in the subgroup of patients with poor respiratory function and in particular with underlying interstitial lung disease, there is a risk of fatal radiation pneumonitis (0.5-1.2%), and extra care must be taken [15]. Clinicians should be aware of the risk of other complications, such as rib fracture, intercostals neuralgia, pleural effusion, liver dysfunction, and brachial plexopathy. Furthermore, attention should be paid to extrapulmonary complications with central tumors close to the mediastinum. There have been reports of fatal hemoptysis [16,17] and fatal esophageal ulcers [18]. Appropriate risk management is essential in central lung cancers where irradiation of the mediastinum (heart/large artery, trachea/bronchi, and esophagus) is unavoidable.

3. Clinical trials

In Japan, a multicenter collaborative clinical trial, the "JCOG 0403 phase II clinical trial of SBRT for T1N0M0 non-small cell lung cancer" took place in 15 facilities throughout Japan. The trial evaluated the efficacy and safety of SBRT for T1N0M non-small lung cancer cases in both operable and inoperable cases. On the one hand, with cases unfit for standard surgery, the question is whether current standard therapy with a total dose of 60-70 Gy, at 2 Gy per day should be replaced. On the other hand, where surgery is possible but refused, the question is whether clinical outcomes equal to surgery can be achieved. The primary endpoint is the 3-year survival rate with secondary endpoints being the overall survival rate, the progression-free survival period, the type of recurrence, and adverse events. The treatment method comprises a total radiation dose of 48 Gy at 12 Gy per day per fraction, three or four times per week for a total of four fractions, with the total treatment period within four to eight days. The results of the operable (but rejected) cases, reported in 2010, showed that although majority of subjects were elderly individuals with a mean age of 79 years, the 3-year survival rate was 76% and the 3-year local control rate calculated as per the Radiation Therapy Oncology Group (RTOG) was 86%. There were very few adverse events over grade 3 (6%). In 2012, the results of the inoperable cases, also using elderly subjects with a mean age of 78 years, were reported. Here the 3-year survival rate was 60%; the 3-year local control rate was 88% with no grade 5 adverse events.

The RTOG 0239 results were reported in the USA in 2009. This clinical trial tested 60 Gy by 3 fractions for the purpose of local control in T1-3N0M0 inoperable lung cancers < 5 cm in size. The median observation period was 36 months, and there was a high local control rate (recurrence within the planning target volume) of 98% at 3 years. However, although there were no grade 5 adverse events, 4% were grade 4 and 24% were grade 3.

In the USA, studies currently underway include the RTOG 0618 on stereotactic irradiation (excluding partial response cases for local effectiveness) for operable lung cancer, the RTOG 0813 dose escalation study from 10 Gy×5 fractions for central hilar lung cancer, and the RTOG 0915 study comparing 12 Gy×4 fractions against 34 Gy×1. Furthermore, in Europe, a scandinavian stereotactic precision and conventional radiotherapy evaluation (SPACE) trial comparing 15

Gy×3 fractions against 2 Gy×35 fractions is currently underway.

Randomized controlled studies between surgery and SRT, including the commencement of American College of Surgeons Oncology Group (ACOSG)/RTOG trial and the randomized study to compare cyberknife to surgical Resection in stage I non-small cell lung cancer (STARS) trial are underway

The Outlook of SBRT

1. Screening and detection of early-stage lung cancer cases

Recent breakthroughs in CT imaging technology paved the way for the discovery of ground glass opacity (GGO) early-stage lesions in the lung. The only current option for such lesions is to obtain a definite diagnosis by surgery. However, it is common for patients with these lesions to be unsuitable for radical surgery because of concurrent lung disease. Studies are needed in which surgery and SBRT are compared for GGO lesions that expand during observation [19].

2. Cases with poor respiratory function

SBRT is often used for patients with poor respiratory function who are considered unsuitable for surgery. Of these patients, only those with chronic obstructive pulmonary disease are not at high risk of radiation pneumonitis following irradiation; therefore, SBRT is considered suitable. However, there is no consensus on the possibility of SRT for patients with any degree of impaired pulmonary function. An analysis of these adaptive criteria is anticipated. In cases with active interstitial pneumonia, there have been many reports of fatal irradiation pneumonitis, and it is generally accepted that they should be excluded from treatment.

3. Hilar lung cancer

When lung cancer develops near the pulmonary hilum, the treatment raises the risk of radiation exposure to key structures, such as the central trachea and bronchi, the esophagus, the pulmonary artery, and the spinal cord. When the tolerance dose is exceeded in these organs, there is the risk of massive hemorrhage because of ulcers in the trachea or bronchi and peripheral bronchial occlusion [16,17]. However, there is a report of no complications with standard high-dose irradiation of 10-15 Gy as far as keeping normal tissue dose constraints [20]. Clinical trials are underway with the aim of finding optimal radiation doses.

4. Expanding the indication toward advanced lung cancer

In advanced-stage lung cancer, the irradiation volume increases, meaning that it is difficult to apply SBRT technology in its current form. However, after 60-70 Gy of 3D irradiation, it may be possible to conduct additional SBRT limited to the remaining tumor. Factors that influence additional radiation exposure include volume effect, fractionation effect, and total treatment duration. Total radiation dose distribution, including these biological factors, needs to be introduced into treatment planning in the future.

5. Four-dimensional radiotherapy planning

Future planning of 4D treatment should take into consideration time factors in existing geometric plans of 3D treatment. For example, even if the same dose of radiation is administered, the therapeutic effects differ greatly depending on the fractionated radiation dose and treatment duration. Furthermore, the final treatment plan may differ depending on the sensitivity to the initial irradiation. Ideally, treatment planning would take place before each irradiation. Gating and tracking are referred to as 4D treatment, but a new 4D treatment plan, including 4D CT, is expected in the future.

6. Development of new IGRT equipment

Current advances in mechanical engineering are outstanding. The IRGT devices are new image capture devices introduced into the irradiation room that reflect images captured before and after treatment. Several devices have been developed and employed clinically: the Hokkaido University real-time tumor-tracking radiotherapy irradiation device with on board imaging on the LINAC, a new irradiation device by Varian and Elekta, Cyberknife, Hyperknife (precession motion irradiation), Tomotherapy, and Vero. Development of these new irradiation devices may enable the future development of innovative irradiation techniques. Remarkable treatment outcomes have been reported in ion beam radiotherapy [21], and a comparative study against X-rays is awaited.

7. New indications for SBRT

In Japan, SBRT is covered by public health insurance and is used for patients with primary lung cancer, metastatic lung cancer, primary liver cancer, metastatic liver cancer and

arteriovenous malformation of the spinal cord.

There are treatment results for roughly 300 cases of liver tumors in Japan. However, radical resection, transcatheter arterial chemoembolization, local ethanol injection, and local ablation using radio frequency waves and microwaves are already conducted in everyday clinical practice. The treatment indications for SBRT in comparison to these established methods of treatment need better definition and guidelines. In the USA, an RTOG clinical trial is underway to determine the dose of radiation in SBRT suitable for primary liver cancer.

In addition to these diseases covered by health insurance, SBRT technology is extremely useful for any lesion limited to a local site. Therefore, renal cancers, adrenal gland tumors, paravertebral tumors, prostate cancer, and pancreatic cancer are being targeted [22].

Conclusion

Radiation therapy is currently advancing from 3D to 4D treatment modalities using IGRT technique. In the future, we can look forward to the development and clinical application of high-precision radiotherapy, especially in SBRT.

Conflicts of Interest

Conflict of interest relevant to this article was not reported.

References

1. Blomgren H, Lax I, Goranson H, Krapelien T, Nilsson B, Naslund I, et al. Radiosurgery for tumors in the body: clinical experience using a new method. J Radiosurg. 1998;1;63-74.
2. Uematsu M, Shioda A, Tahara K, Fukui T, Yamamoto F, Tsumatori G, et al. Focal, high dose, and fractionated modified stereotactic radiation therapy for lung carcinoma patients: a preliminary experience. Cancer. 1998;82:1062-70.
3. Onishi H, Kuriyama K, Komiyama T, Tanaka S, Sano N, Aikawa Y, et al. A new irradiation system for lung cancer combining linear accelerator, computed tomography, patient self-breath-holding, and patient-directed beam-control without respiratory monitoring devices. Int J Radiat Oncol Biol Phys. 2003;56:14-20.
4. Negoro Y, Nagata Y, Aoki T, Mizowaki T, Araki N, Takayama K, et al. The effectiveness of an immobilization device in conformal radiotherapy for lung tumor: reduction of respiratory tumor movement and evaluation of the daily setup accuracy. Int J Radiat Oncol Biol Phys. 2001;50:889-98.
5. Uematsu M, Shioda A, Suda A, Fukui T, Ozeki Y, Hama Y, et al. Computed tomography-guided frameless stereotactic radiotherapy for stage I non-small cell lung cancer: a 5-year experience. Int J Radiat Oncol Biol Phys. 2001;51:666-70.
6. Nagata Y, Takayama K, Matsuo Y, Norihisa Y, Mizowaki T, Sakamoto T, et al. Clinical outcomes of a phase I/II study of 48 Gy of stereotactic body radiotherapy in 4 fractions for primary lung cancer using a stereotactic body frame. Int J Radiat Oncol Biol Phys. 2005;63:1427-31.
7. Onimaru R, Shirato H, Shimizu S, Kitamura K, Xu B, Fukumoto S, et al. Tolerance of organs at risk in small-volume, hypofractionated, image-guided radiotherapy for primary and metastatic lung cancers. Int J Radiat Oncol Biol Phys. 2003; 56:126-35.
8. Arimoto T, Usubuchi H, Matsuzawa T. Small volume multiple non-coplanar arc radiotherapy for tumors of the lund, head and neck and the abdominopelvic region. In: Lemke HU, editor. CAR'98 Computer assisted radiology and surgery. Tokyo: Elsevier; 1998. p. 257-61.
9. Timmerman R, Paulus R, Galvin J, Michalski J, Straube W, Bradley J, et al. Stereotactic body radiation therapy for inoperable early stage lung cancer. JAMA. 2010;303:1070-6.
10. Wulf J, Haedinger U, Oppitz U, Thiele W, Mueller G, Flentje M. Stereotactic radiotherapy for primary lung cancer and pulmonary metastases: a noninvasive treatment approach in medically inoperable patients. Int J Radiat Oncol Biol Phys. 2004;60:186-96.
11. Xia T, Li H, Sun Q, Wang Y, Fan N, Yu Y, et al. Promising clinical outcome of stereotactic body radiation therapy for patients with inoperable Stage I/II non-small-cell lung cancer. Int J Radiat Oncol Biol Phys. 2006;66:117-25.
12. Baumann P, Nyman J, Hoyer M, Wennberg B, Gagliardi G, Lax I, et al. Outcome in a prospective phase II trial of medically inoperable stage I non-small-cell lung cancer patients treated with stereotactic body radiotherapy. J Clin Oncol. 2009;27: 3290-6.
13. Fowler JF. Sensitivity analysis of parameters in linear-quadratic radiobiologic modeling. Int J Radiat Oncol Biol Phys. 2009;73:1532-7.
14. Onishi H, Araki T, Shirato H, Nagata Y, Hiraoka M, Gomi K, et al. Stereotactic hypofractionated high-dose irradiation for stage I nonsmall cell lung carcinoma: clinical outcomes in 245 subjects in a Japanese multiinstitutional study. Cancer. 2004; 101:1623-31.
15. Takeda A, Enomoto T, Sanuki N, Nakajima T, Takeda T, Sayama K, et al. Acute exacerbation of subclinical idiopathic pulmonary fibrosis triggered by hypofractionated stereotactic body radiotherapy in a patient with primary lung cancer and slightly focal honeycombing. Radiat Med. 2008;26:504-7.
16. Nagata Y, Hiraoka M, Mizowaki T, Narita Y, Matsuo Y, Norihisa Y, et al. Survey of stereotactic body radiation therapy in Japan by the Japan 3-D Conformal External Beam Radiother-

apy Group. Int J Radiat Oncol Biol Phys. 2009;75:343-7.
17. Corradetti MN, Haas AR, Rengan R. Central-airway necrosis after stereotactic body-radiation therapy. N Engl J Med. 2012; 366:2327-9.
18. Timmerman R, McGarry R, Yiannoutsos C, Papiez L, Tudor K, DeLuca J, et al. Excessive toxicity when treating central tumors in a phase II study of stereotactic body radiation therapy for medically inoperable early-stage lung cancer. J Clin Oncol. 2006;24:4833-9.
19. Inoue T, Shimizu S, Onimaru R, Takeda A, Onishi H, Nagata Y, et al. Clinical outcomes of stereotactic body radiotherapy for small lung lesions clinically diagnosed as primary lung cancer on radiologic examination. Int J Radiat Oncol Biol Phys. 2009;75:683-7.
20. Chang JY, Balter PA, Dong L, Yang Q, Liao Z, Jeter M, et al. Stereotactic body radiation therapy in centrally and superiorly located stage I or isolated recurrent non-small-cell lung cancer. Int J Radiat Oncol Biol Phys. 2008;72:967-71.
21. Miyamoto T, Baba M, Yamamoto N, Koto M, Sugawara T, Yashiro T, et al. Curative treatment of Stage I non-small-cell lung cancer with carbon ion beams using a hypofractionated regimen. Int J Radiat Oncol Biol Phys. 2007;67:750-8.
22. Nagata Y, Wulf J, Lax I, Timmerman R, Zimmermann F, Stojkovski I, et al. Stereotactic radiotherapy of primary lung cancer and other targets: results of consultant meeting of the International Atomic Energy Agency. Int J Radiat Oncol Biol Phys. 2011;79:660-9.

Hepatology Research

Hepatology Research 2013; 43: 717–727 doi: 10.1111/hepr.12007

Original Article

Dynamic computed tomography appearance of tumor response after stereotactic body radiation therapy for hepatocellular carcinoma: How should we evaluate treatment effects?

Tomoki Kimura,[1] Shigeo Takahashi,[1] Masahiro Kenjo,[1] Ikuno Nishibuchi,[1] Ippei Takahashi,[1] Yuki Takeuchi,[1] Yoshiko Doi,[1] Yuko Kaneyasu,[1] Yuji Murakami,[1] Yoji Honda,[2] Hiroshi Aikata,[2] Kazuaki Chayama[2] and Yasushi Nagata[1]

[1]*Department of Radiation Oncology, Graduate School of Biomedical Sciences, Hiroshima University, Hiroshima, Japan and* [2]*Department of Medicine and Molecular Science, Division of Frontier Medical Science, Programs for Biomedical Research, Graduate School of Biomedical Sciences, Hiroshima University, Hiroshima, Japan*

Aim: To evaluate the dynamic computed tomography (CT) appearance of tumor response after stereotactic body radiation therapy (SBRT) for hepatocellular carcinoma (HCC) and reconsider response evaluation criteria for SBRT that determine treatment outcomes.

Methods: Fifty-nine patients with 67 tumors were included in the study. Of these, 56 patients with 63 tumors underwent transarterial chemoembolization using lipiodol prior to SBRT that was performed using a 3-D conformal method (median, 48 Gy/four fractions). Dynamic CT scans were performed in four phases, and tumor response was evaluated by comparing tumor appearance on CT prior SBRT and at least 6 months after SBRT. The median follow-up time was 12 months.

Results: The dynamic CT appearance of tumor response was classified into the following: type 1, continuous lipiodol accumulation without early arterial enhancement (26 lesions, 38.8%); type 2, residual early arterial enhancement within 3 months after SBRT (17 lesions, 25.3%); type 3, residual early arterial enhancement more than 3 months after SBRT (19 lesions, 28.4%); and type 4, shrinking low-density area without early arterial enhancement (five lesions, 7.5%). Only two tumors with residual early arterial enhancement did not demonstrate remission more than 6 months after SBRT.

Conclusion: The dynamic CT appearance after SBRT for HCC was classified into four types. Residual early arterial enhancement disappeared within 6 months in most type 3 cases; therefore, early assessment within 3 months may result in a misleading response evaluation.

Key words: dynamic computed tomography appearance, hepatocellular carcinoma, stereotactic body radiation therapy

INTRODUCTION

HEPATOCELLULAR CARCINOMA (HCC) is closely associated with hepatitis B virus (HBV) or hepatitis C virus (HCV) infections and the increasing prevalence of viral infections has led to an increased incidence of HCC. The curative therapy for HCC involves surgery including resection or transplantation.[1,2] However, only 10–30% patients initially presenting with HCC would be eligible for surgery either due to liver dysfunction, underlying cirrhosis or presence of multifocal tumors arising from viral infection.[3] For such patients, locoregional therapies such as ablative therapies or transarterial chemoembolization (TACE) are recommended.[1,2] Radiation therapy is a locoregional therapy that can be considered as an alternative to ablation/TACE or when these therapies have failed.[1] Recently, advances in imaging and radiation techniques that deliver high doses of radiation to focal HCC have helped to avoid

Correspondence: Dr Tomoki Kimura, Department of Radiation Oncology, Graduate School of Biomedical Sciences, Hiroshima University, 1-2-3 Kasumi, Minami-ku, Hiroshima City 734-8551, Japan. Email: tkkimura@hiroshima-u.ac.jp

This work was partly presented at the 53rd Annual Meeting of American Society for Therapeutic Radiology and Oncology (ASTRO), Miami, FL, USA, October 1–5 2011.

Conflict of interest: none.

Received 1 July 2012; revision 30 September 2012; accepted 15 October 2012.

radiation-induced liver damage (RILD). Several studies have reported good treatment outcomes with either stereotactic body radiation therapy (SBRT) or particle therapy with or without TACE for HCC,[4–7] and experience with radiation therapy for HCC has increased rapidly during the past decade.[8] These reports used various methods, such as the Response Evaluation Criteria in Solid Tumors (RECIST),[9] the World Health Organization (WHO) response evaluation criteria,[10] and dynamic CT with or without tumor enhancement[5] to evaluate tumor response. However, no significant progress has been made in establishing a consensus from the various studies that have evaluated the response of HCC to SBRT or particle therapy. Furthermore, no detailed studies have reported the use of CT to monitor tumor response after SBRT or particle therapy. It is extremely important to record the CT appearance at regular intervals to accurately evaluate tumor response because HCC demonstrates changes with time after SBRT.

The purpose of our study was to evaluate the dynamic CT appearance of tumor response after SBRT in conjunction with TACE for HCC and to reconsider response evaluation criteria for SBRT to determine treatment outcomes.

METHODS

Patient background

FROM MARCH 2002 to December 2011, 73 patients with 88 tumors underwent SBRT at our institution. Our study included 59 patients with 67 tumors who were analyzed using dynamic CT for more than 6 months after SBRT. There were 37 men and 22 women with a median age of 71 years (range, 49–90), including five patients with chronic hepatitis B and 47 patients with chronic hepatitis C. Six patients simultaneously underwent SBRT for two tumors each and two patients each with a solitary tumor were treated at different times. The inclusion criteria for curative SBRT were as follows: (i) patients over 20 years of age; (ii) an Eastern Cooperative Oncology Group Performance Status (ECOG PS) of 0–2; (iii) Child–Pugh score A or B; (iv) less than three HCC nodules, each up to 50 mm in diameter, without portal venous thrombosis or extrahepatic metastases; (v) inoperable patients because of their poor general condition or refusal of surgery; and (vi) patients unsuitable for radiofrequency ablation (RFA) because of tumor location (e.g. on the liver surface and near the porta hepatis), invisibility of tumor on ultrasonography or bleeding tendency. The exclusion criterion was presence of uncontrolled ascites. The majority of patients had previously undergone surgery or ablation therapies, and SBRT was recommended when these options were limited by technical difficulties or if the patient was inoperable or refused surgery. The clinical characteristics of the patients including age, sex, type of viral infection, Child–Pugh score, primary tumor location and size, ECOG PS and previous treatments are summarized in Table 1.

Hepatocellular carcinoma was diagnosed by its characteristic appearance of early enhancement in the arterial phase and hypodensity in the portal venous phase, which was revealed in most of the patients using either dynamic CT or angiography combined with CT. However, for five patients in whom these CT appearance were not observed, HCC was diagnosed histologically.

Treatment procedure

Before SBRT, 56 patients with 63 HCC underwent TACE using iodized lipiodol (lipiodol). Anticancer chemotherapies, such as epirubicin, cisplatin combined with lipiodol (7–70 mg/body at a concentration of 10 mg/mL lipiodol) or miriplatin mixed with lipiodol (20–80 mg/body at a concentration of 20 mg/mL lipiodol), administrated by injecting the drug into the hepatic artery feeding a segment or subsegments of the target tumor. The selected dose was based on tumor size and liver function. A small amount of gelatin sponge particles was used to induce embolization until the flow through the feeding artery was markedly decreased. The median time interval between TACE and SBRT was 1 month (range, 1–7). The interval was 1–2 months in most of the patients, but was 6–7 months in four patients. They were treated only with TACE because two patients were elderly and had some complications, and the other two patients wanted to be treated only with TACE at first.

Stereotactic body radiation therapy was performed using a 3-D conformal method in which a single high dose is delivered to the tumor. A vacuum cushion (Vac-Lok; CIVCO, Kalona, IA, USA) was used to immobilize the patient. Respiratory motion was evaluated using an X-ray simulator. If respiratory motion was greater than 5 mm, it was coordinated by either voluntary breath-holding using a spirometer or Abches (APEX Medical, Tokyo, Japan), which is a device that allows the patient to control the respiratory motion of their chest and abdomen. Patients held their breath in the end-expiratory phase because the interbreath-hold reproducibility of organ position in end-expiratory phase was better than that in the end-inspiratory phase.[11] This

Table 1 Patients background

Age	49–90 (median, 71)	Tumor size	3–54 mm (median, 19 mm)
Sex		Tumor location	
Male	37 patients	S1	1 lesion
Female	22 patients	S2	1 lesion
ECOG PS		S3	4 lesions
0	55 patients	S4	12 lesions
1	3 patients	S5	8 lesions
2	1 patient	S6	6 lesions
Type of viral infection		S7	15 lesions
HBV	5 patients	S8	20 lesions
HCV	47 patients	Previous treatment	
NBNC	7 patients	Surgery	21 patients
Child–Pugh class		RFA	17 patients
A	46 patients	PEI	9 patients
B	13 patients	TACE	56 patients
Child–Pugh score			
5	33 patients		
6	13 patients		
7	8 patients		
8≧	5 patients		

ECOG PS, Eastern Cooperative Oncology Group Performance Status; HBV, hepatitis B virus; HCV, hepatitis C virus; NBNC, non-hepatitis B non-hepatitis C; PEI, percutaneous ethanol injection; RFA, radiofrequency ablation; TACE, transcatheter arterial chemoembolization.

method was employed in 55 patients with 62 tumors. The free-breathing method was used in two patients with three tumors, and respiratory-gating using the Real-time Position Management (RPM) system (Varian Medical Systems, Palo Alto, CA, USA) was used in two patients with two tumors. For simulation, dynamic CT scans (Lightspeed QX/I; GE Medical Systems, Waukesha, WI, USA), including non-enhanced and contrast-enhanced scans, were performed in four phases, before contrast enhancement, and arterial, portal and venous phases. CT was performed using bolus injection of non-ionic iodinated contrast material (100 mL at a rate of 3 mL/s). CT volume data in the arterial phase were transferred to a 3-D treatment planning system (Pinnacle[3] ver. 9.0; Phillips Medical Systems, Fitchburg, WI, USA). Gross tumor volume (GTV) was defined as the volume of tumor containing the remains of lipiodol used with TACE and from early enhancement in the arterial phase of dynamic CT. A clinical target volume (CTV) margin of 3 mm was usually added to GTV for subclinical invasion. A planning target volume (PTV) margin of 5–8 mm, which included the reproducibility of respiratory motion and setup error to CTV, was usually added. Eight non-coplanar ports were selected in all patients, including four or five coplanar beams and three or four non-coplanar beams in a direction that avoided the stomach, intestine, gall bladder and spine, if possible. The prescribed dose and fractionations were 60 Gy/eight fractions in 10 tumors, 50 Gy/five fractions in five tumors, 40 Gy/four fractions in one tumor and 48 Gy/four fractions in 51 tumors. Beams were delivered using 6–10-MV photons of linear accelerator (CLINAC 2300 C/D or iX; Varian Medical Systems, Palo Alto, CA, USA) that delivered 600 monitor units/min so that the duration of breath-holding could be 15 s or less for each treatment field.

Evaluation

Follow-up dynamic CT was performed every 1–3 months after SBRT. Serum HCC-specific tumor markers including α-fetoprotein were also investigated every 1–2 months. If the level of the tumor markers were increased significantly, additional dynamic CT was performed. Dynamic CT of the entire liver was performed using multidetector row helical CT (16 channels, Light Speed Ultra 16 or 64 channels, Light Speed VCT; GE, Milwaukee, WI, USA) with a 5-mm reconstructed slice width and a 5-mm slice interval. The scanning parameters were 120 kV, Auto mA (noise index, 10), 5-mm section thickness, 1.375 beam pitch, and a 0.7 or 0.4 rotation speed.

Images were obtained in four phases, which included before-contrast enhancement, early arterial, late arterial and portal venous phase after injection of 100 mL of non-ionic iodinated contrast material at a rate of 4 mL/s using an automatic injector. Hepatic arterial, portal venous and equilibrium phase scans were performed for 15–17 s, 45–47 s and 145–147 s, respectively, after triggering using an automatic bolus-tracking program. The dynamic CT appearance was evaluated using a soft-tissue window (level, 40 HU; width, 200 HU), and was confirmed following a consensus between one of the authors (T. K.) and two radiologists for each of the 67 tumors.

The dynamic CT appearance of tumor response and the relationship between tumor appearance and clinical features were evaluated from these results. In addition, local treatment results, such as the local progression-free survival rate (LPFS) and local control rate (LCR), were compared based on several evaluation methods. Treatment-related toxicities were evaluated by the Common Terminology Criteria for Adverse Events (CTCAE) ver. 4. 0.

Median follow up at the time of evaluation was 12 months (range, 6 –45).

Statistical methods

Univariate analysis using the Mantel–Haenszel χ^2-test or Student's *t*-test and multivariate analyses using the logistic regression test for comparison of statistical significance were used. The LPFS and LCR were calculated using the Kaplan–Meier method. All statistical analyses were performed using StatMate for Windows (StatMate ver. 4.01; ATMS, Tokyo, Japan). Statistical significance was defined as $P < 0.05$.

RESULTS

Dosimetric factors

THE MEDIAN GTV and PTV were 2.9 cc (range, 0.2–38.8) and 27.5 cc (range, 5.5–132.6), respectively. The median dose of PTV was 47.6 Gy (range, 39.4–60.0) and the median percentage of PTV dose relative to the isocenter dose was 98.5% (range, 95.6–102.7%) which is considered to be good dose coverage to PTV.

Dynamic CT appearance of tumor response

The dynamic CT appearance of tumor response was classified into the following four types: type 1, continuous lipiodol accumulation without early arterial enhancement (26 tumors, 38.8%) (Fig. 1); type 2, residual early arterial enhancement within 3 months after SBRT (17 tumors, 25.3%) (Fig. 2); type 3, residual early arterial enhancement more than 3 months after SBRT (19 tumors, 28.4%) (Fig. 3); and type 4, shrinking low-density area without early arterial enhancement after SBRT (five tumors, 7.5%) (Fig. 4). None of the tumors increased in size during the follow-up period. Two tumors (3.0%) demonstrated residual early arterial enhancement for more than 6 months after SBRT; however, most of these features disappeared within 6 months.

Relationship between the dynamic CT appearance of tumor response and clinical features

Table 2 presents the results of univariate analysis between the dynamic CT appearance of tumor response and clinical features, such as Child–Pugh class, sex, age, total dose, PTV, tumor location, history of resection and duration of initial treatment. *P*-value was defined as the clinical factors in each type of dynamic CT appearance as compared to those in the other types. The clinical features of patients with each of the four types of dynamic CT appearance were compared. Significant differences were observed in Child–Pugh class for type 4, sex for type 3, total dose and PTV for types 1 and 4, history of resection for type 4, and duration of initial treatment for type 2.

Table 3 presents the results of multivariate analysis between the dynamic CT appearance of tumor response and clinical features that showed significant differences in univariate analysis. History of resection in type 1 was the only significant factor in multivariate analysis.

Local treatment results

Figure 5(a,b) shows LPFS and LCR, respectively, based on the evaluation criteria 1–3 (shown below). An event was defined as local tumor progression and death in LPFS and local tumor progression in LCR; death without local tumor progression was censored. Evaluation criteria were: (1) local tumor progression defined as growth of an irradiated tumor and presence of a hypervascular nodule adjacent to the treated area; (2) local tumor progression defined as growth of an irradiated tumor, residual early arterial enhancement for more than 3 months and presence of a hypervascular nodule adjacent to the treated area; and (3) local tumor progression defined as growth of an irradiated tumor, residual early

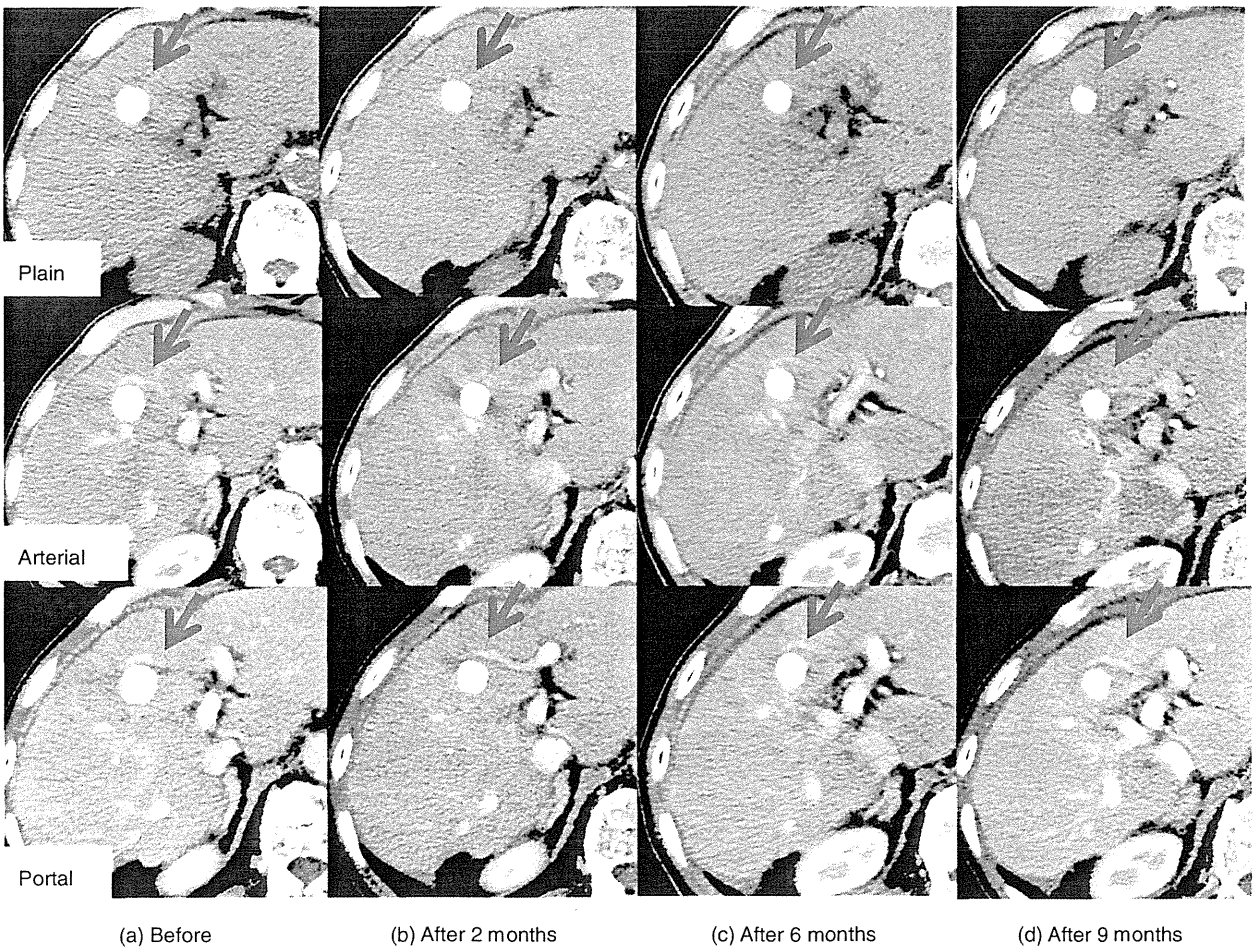

Figure 1 Dynamic computed tomography appearance of tumor response type 1 (plain, arterial and portal phase in case 37). (a) Before stereotactic body radiation therapy; (b) 2 months after; (c) 6 months after, and (d) 9 months after. Note the continuous presence of dense lipiodol accumulation without early arterial enhancement in all phases (red arrow).

arterial enhancement for more than 6 months and presence of a hypervascular nodule adjacent to the treated area.

Significant differences in LPFS were observed between evaluations 1 and 2 and between evaluations 2 and 3 ($P = 0.0089$ and 0.0242, respectively). Significant differences in LCR were observed between evaluations 1 and 2 and between evaluations 2 and 3 ($P < 0.0001$ and 0.0004, respectively).

We also evaluated the tumor response according to the Response Evaluation Criteria in Cancer of the Liver (RECICL).[12] Type 1 and 2 were equivalent to complete response (CR). Most type 3 tumors were also equivalent to CR because residual early arterial enhancement disappeared within 6 months. Two type 3 tumors demonstrated residual early arterial enhancement for more than 6 months after SBRT, however, the reduction rate of these two tumors was more than 50%, equivalent to partial response (PR). All five type 4 tumors were also equivalent to PR because of its reduction rate of more than 50%. From these results, response rate (CR + PR) was 100% and CR rate was 89.6% (60/67 tumors) according to RECICL in this study.

Treatment-related toxicities

None of the patients experienced new acute hematological or physical toxicities of more than grade 3 after TACE. However, seven patients (11.9%) developed grade 3 toxicities, such as bilirubin and ascites eleva-

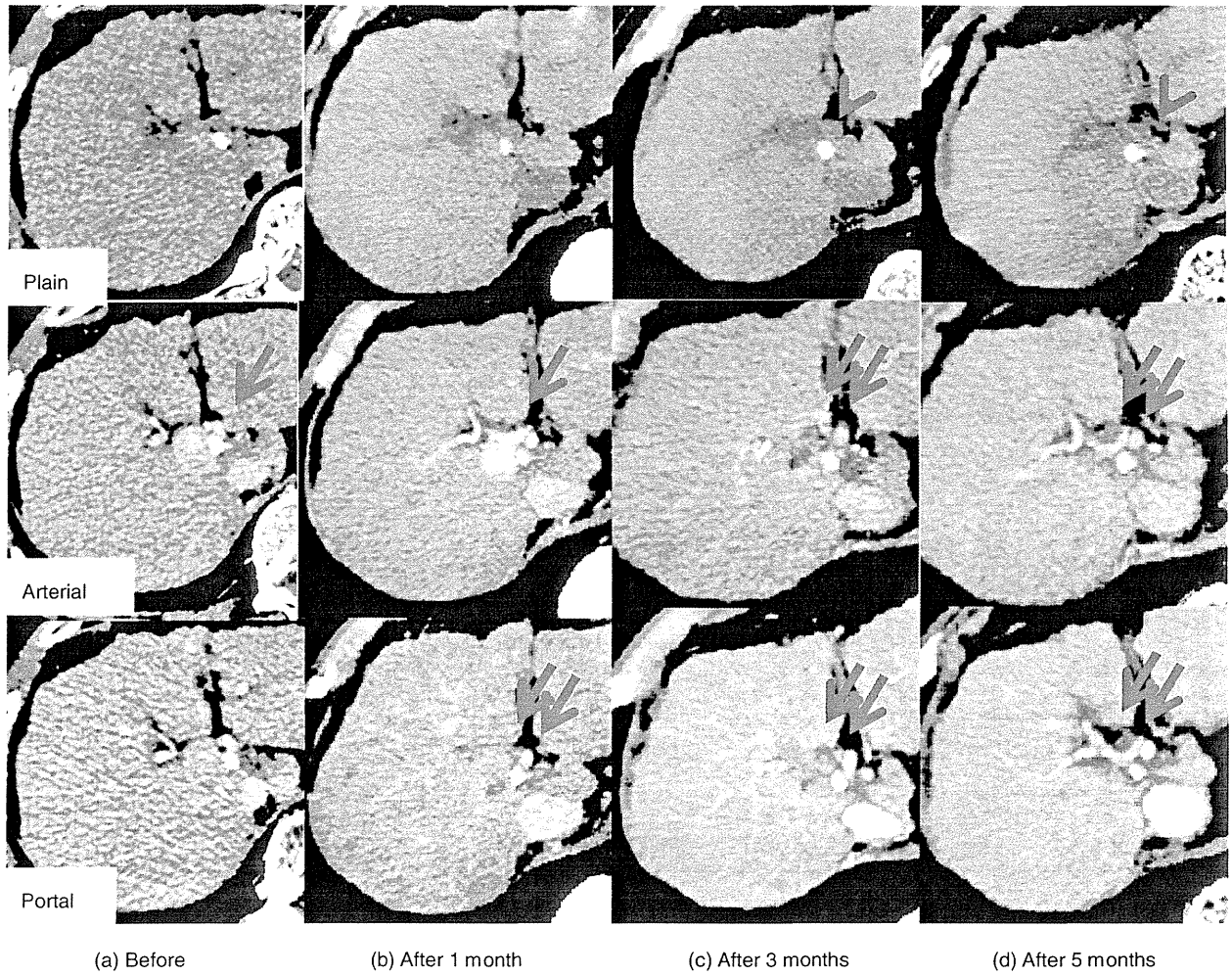

Figure 2 Dynamic computed tomography appearance of tumor response type 2 (plain, arterial and portal phase in case 9). (a) Before stereotactic body radiation therapy (SBRT); early arterial enhancement and partial residual lipiodol were observed (red arrow). (b) One month after SBRT, early arterial enhancement was still present (red arrow). Hypodensity of this tumor changed in the portal venous phase (two red arrows). (c) Three and (d) 5 months after SBRT, early arterial enhancement was no longer evident and hypodensity changed (two red arrows). Residual lipiodol accumulation is still noted (red arrow head).

tions, and one and six patients were in Child–Pugh classes A and B, respectively. None of the patients experienced RILD.

DISCUSSION

SEVERAL AUTHORS HAVE reported the typical CT appearance of RILD after SBRT; typical areas of high-dose radiation reaction appear hypodense in most non-enhanced scans and hyperdense in contrast-enhanced delayed scans.[13,14] These findings could be based on the histopathological features of veno-occlusive disease (VOD), which was recognized as radiation injury to the liver.[15,16] Olsen *et al.* described VOD with marked sinusoidal congestion and venous damage in two patients who underwent exploratory surgery following SBRT.[15] Willemart *et al.* reported that the appearance of hypodensity in the portal venous phase that becomes hyperdense in the delayed phase could be explained by decreased vascular perfusion and reduced hepatic venous drainage with subsequent stasis of the contrast medium.[16] However, the appearance of a tumor response in CT is different from that of RILD, and a tumor response after SBRT has not been reported in

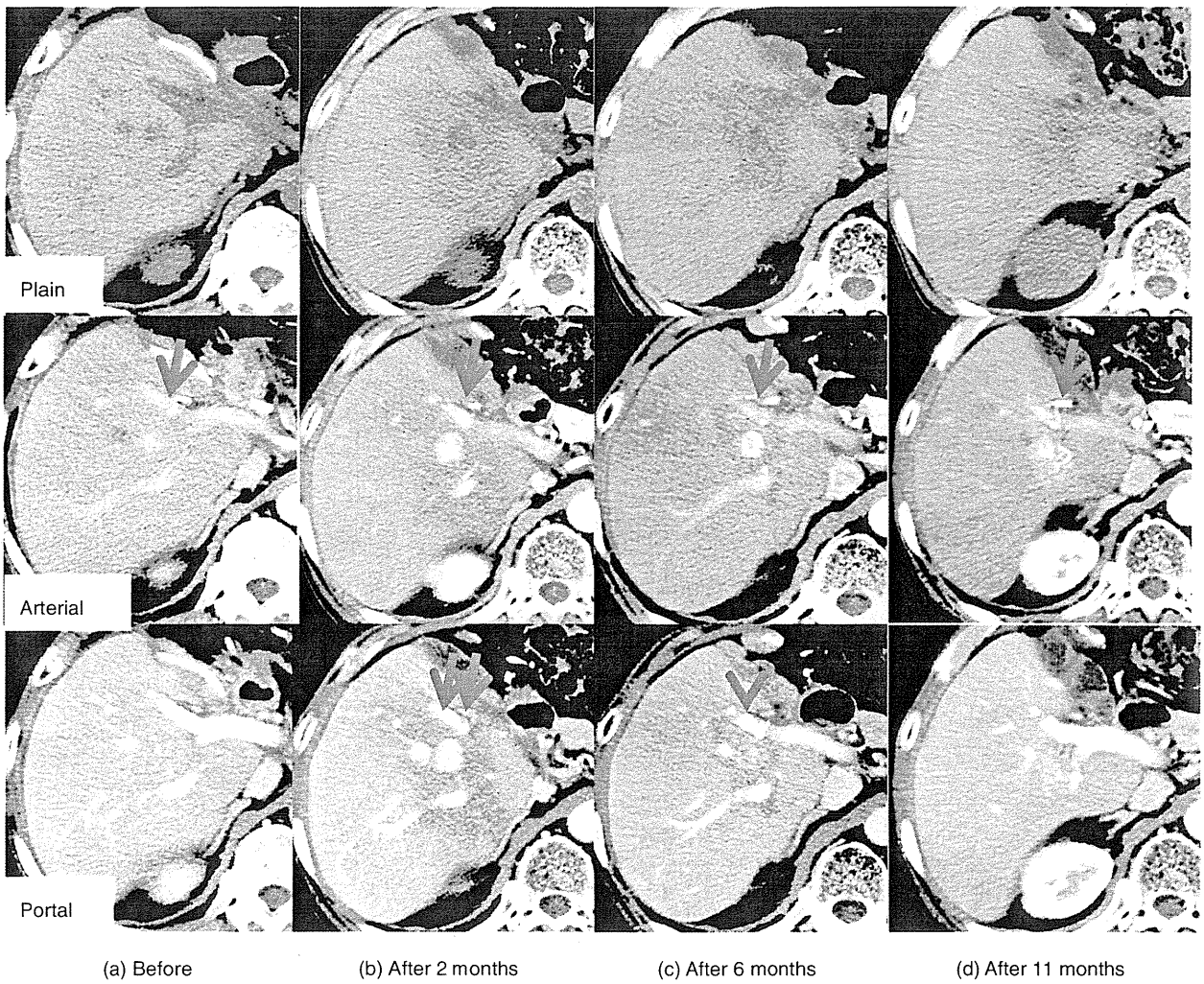

Figure 3 Dynamic computed tomography appearance of tumor response type 3 (plain, arterial and portal phase in case 39). (a) Before stereotactic body radiation therapy (SBRT), early arterial enhancement is visible (red arrow). (b) Two and (c) 6 months after SBRT, early arterial enhancement is more evident than that before SBRT in arterial (red arrow) and portal phase (two red arrows). (d) Eleven months after SBRT, although shrinking, it remains (red arrow).

detail. In this study, we classified the dynamic CT appearance of tumor response into four types. Most patients underwent TACE using lipiodol before SBRT and demonstrated a combination of residual early arterial enhancement with or without residual lipiodol. Therefore, early arterial enhancement was a characteristic dynamic CT finding for viable HCC, and the existence of residual early arterial enhancement after SBRT may indicate residual or recurrent HCC histologically.

Evaluation of the relationship between the dynamic CT appearance of tumor response and clinical features showed that history of resection in type 1 was the only significant factor in multivariate analyses. Sanuki-Fujimoto *et al.* described the CT appearance of RILD after SBRT and demonstrated that liver tissue with preserved function was more likely to be well enhanced in the delayed phase of dynamic CT.[14] However, our analysis of tumor response did not demonstrate a significant relationship between Child–Pugh class and residual early arterial enhancement observed in types 2 and 3.

Although RECIST and WHO criteria are widely used to evaluate solid tumor responses to chemotherapy or radiation therapy,[9,10] they may be inappropriate for evaluating tumor response to locoregional therapies

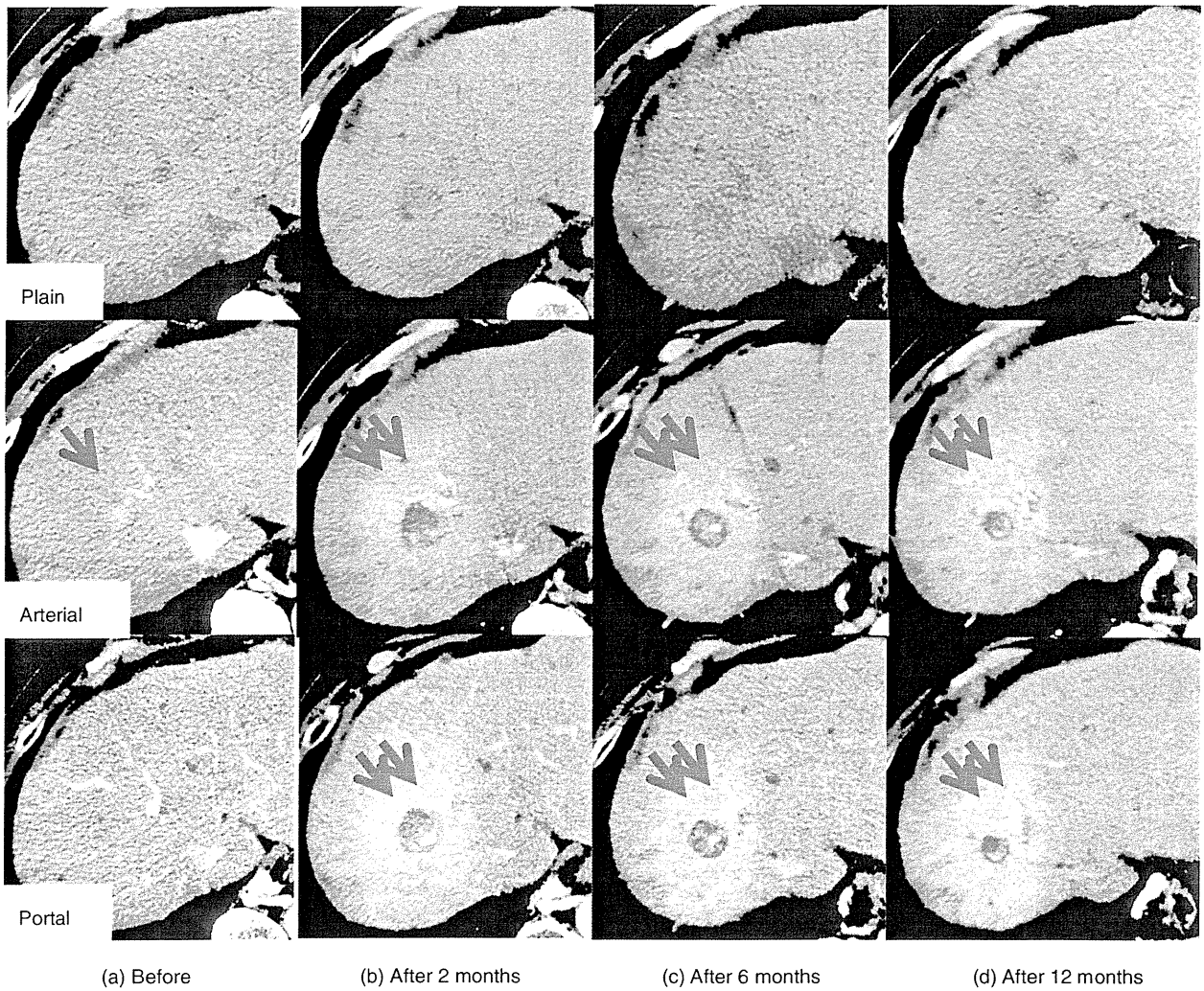

Figure 4 Dynamic computed tomography appearance of tumor response type 4 (plain, arterial and portal phase in case 11). (a) Before stereotactic body radiation therapy (SBRT), early arterial enhancement is visible (red arrow). (b) Two, (c) 6 and (d) 12 months after SBRT, hypodensity of the tumor changed and the tumor shrank without early arterial enhancement in arterial and portal phase (two red arrows). Radiation-induced liver damage is visible around the tumor.

such as ablation therapies and TACE in most patients with HCC because they only rely on tumor size reduction as a measure of effect and do not consider any necrotizing effects or tumor blood flow. RECICL were proposed by the Liver Cancer Study Group of Japan.[12] This study group addressed these concerns by including criteria that consider the biological characteristics of HCC. Tumor necrosis is regarded as a direct effect of treating a target tumor, and the dense accumulation of lipiodol is regarded as necrosis. In addition, although RECIST and WHO criteria do not specify the timing when overall treatment outcomes should be assessed, RECICL suggests that the maximum response within 3 months for TACE or local ablative therapies and 6 months for radiotherapy should be regarded as the overall treatment effects. Although the above criteria should be kept in mind for ablative therapies, which typically result in necrosis, most CT appearances after SBRT in our study did not show obvious tumor necrosis. In addition, RECICL may be inappropriate for the evaluation of tumor response by SBRT because the healing stage of ablative therapies and SBRT are different. The

Table 2 Univariate analysis between the dynamic CT appearance of tumor response and clinical features

		Type 1	*P* Uni†	Type 2	*P* Uni	Type 3	*P* Uni	Type 4	*P* Uni
Child–Pugh class	A	21	0.622	15	0.278	14	0.628	2	0.036
	B	5		2		5		3	
Sex	Male	19	0.112	11	0.731	8	0.044	3	0.955
	Female	7		6		11		2	
Age	>75 years	10	0.877	5	0.436	9	0.284	1	0.405
	≤75 years	16		12		10		4	
Total dose	>48 Gy	4	<0.001	6	0.14	3	0.415	2	0.033
	≤48 Gy	22		11		16		3	
Planning target volume	>40 cc	3	0.024	4	0.719	6	5842	5	0.0001
	≤40 cc	23		13		13		0	
Tumor location	Peripheral	24	0.082	12	0.152	15	0.729	4	0.899
	Central	2		5		4		1	
History of resection	+	10	0.877	6	0.842	5	0.242	4	0.04
	−	16		11		14		1	
Duration from first treatment	>12 months	13	0.134	14	0.038	10	0.366	4	0.37
	≤12 months	13		3		9		1	

**P*-value was defined as the clinical factors in each type of dynamic computed tomography (CT) appearance as compared to those in the other types.
†Uni: univariate analysis by the Mantel–Haenzel χ^2-test or Student's *t*-tests.

treatment results in our study were also different according to the evaluation methods, such as RECICL and our criteria including residual early arterial enhancement.

Several authors have reported treatment results of SBRT or particle therapy for HCC and their evaluation methods.[4–7] Andolino *et al.* used RECIST to evaluate tumor response after SBRT on the basis of tumor size.[4] Takeda *et al.* reported that when no tumor enhancement was detected within PTV on enhanced dynamic CT 6 months or more after SBRT, patients were considered to have no relapse.[5] With regard to particle therapies, Fukumitsu *et al.* defined local progression as growth of the irradiated tumor or the appearance of new tumors within the treatment volume after proton therapy.[6] In

Table 3 Multivariate analysis between the dynamic CT appearance of tumor response and clinical features

		Type 1	*P* Multi†	Type 2	*P* Multi	Type 3	*P* Multi	Type 4	*P* Multi
Child–Pugh class	A	21	0.999	15	0.999	14	0.999	2	0.226
	B	5		2		5		3	
Sex	Male	19	0.845	11	0.331	8	0.587	3	0.997
	Female	7		6		11		2	
Total dose	>48 Gy	4	0.505	6	0.5	3	0.999	2	0.307
	≤48 Gy	22		11		16		3	
Planning target volume	>40 cc	3	0.333	4	0.981	6	0.869	5	0.996
	≤40 cc	23		13		13		0	
History of resection	+	10	0.028	6	0.056	5	0.712	4	0.996
	−	16		11		14		1	
Duration from first treatment	>12 months	13	0.104	14	0.056	10	0.773	4	0.998
	≤12 months	13		3		9		1	

**P*-value was defined as the clinical factors in each type of dynamic computed tomography (CT) appearance as compared to those in the other types.
†Multi: multivariate logistic regression analysis.

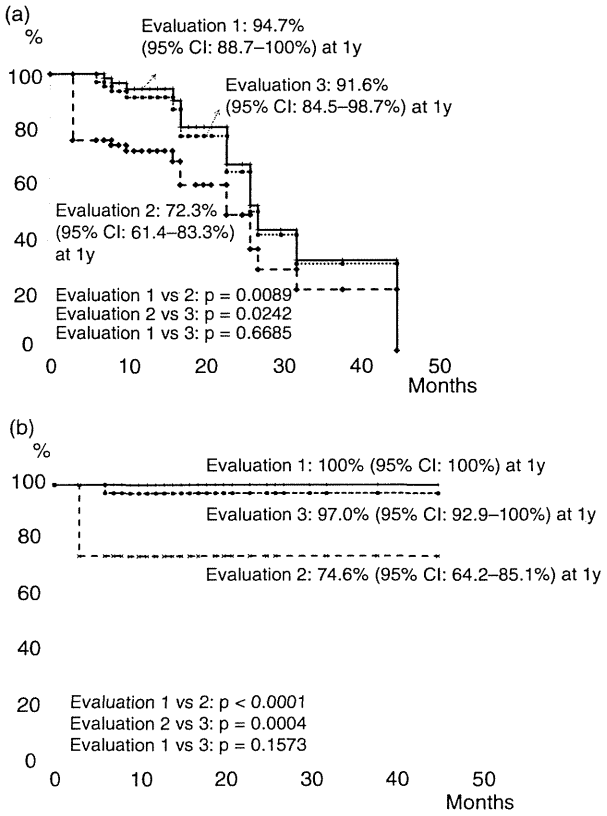

Figure 5 Treatment results of stereotactic body radiation therapy (SBRT) based on the different evaluation criteria. (a) Local progression-free survival rate (LPFS) according to evaluations 1–3. LPFS according to evaluation 2 was significantly lower than that according evaluations 1 and 3. (b) Local control rate (LCR) according to evaluations 1–3. LCR according to evaluation 2 was also significantly lower than that according to evaluation 1 and 3. CI, confidence interval; y, years.

this study, no tumors showed enlargement during the follow-up period, which should be included as a good tumor response among the other criteria described above. Takayasu *et al.* correlated histological and radiological data and indicated that accumulation of lipiodol within the tumor occurred primarily in areas of tumor necrosis.[17] They concluded that dense accumulation of lipiodol was a reliable indicator of necrosis. Based on our results, continuous dense accumulation of lipiodol without early arterial enhancement after SBRT (dynamic CT appearance, type 1) may also be included as a criterion of tumor response. However, the optimal method for evaluating early arterial enhancement after SBRT has not been confirmed. In this study, residual early arterial enhancement for more than 3 or 6 months after SBRT was observed in 19 (28.4%) and two lesions (3.0%), respectively. According to our evaluation methods (described above), residual early arterial enhancement was regarded as local progression. However, most of these findings that were noted for more than 3 months after SBRT disappeared within 6 months. We also observed shrinkage or disappearance of residual early arterial enhancement for more than 6 months after SBRT in two patients at 10 and 11 months. Our results indicate that when residual early arterial enhancement for more than 3 or 6 months was regarded as local progression, the treatment results differed significantly, especially when the treatment outcomes were assessed as early as 3 months after SBRT, which may be too early. Therefore, patient evaluation should be carefully performed. If the treated tumors are not enlarged, tumor markers are within the normal range, and residual early arterial enhancement for more than 6 months is noted, we recommend that an additional follow up should be performed, at least 12 months after SBRT. Other modalities should also be considered, such as gadoxetic acid-enhanced magnetic resonance imaging (Gd-EOB-MRI; GE Healthcare, Chalfont St. Giles, UK) or enhanced (Sonazoid; Daiichi Pharmaceutical, Tokyo, Japan) ultrasound (US) in these cases. However, in dynamic studies of Gd-EOB-MRI or Sonazoid US, appearances were similar to CT; therefore, there were few hepatocytes or Kupffer cells in the irradiated normal liver tissues, including those of HCC. Thus, it may be difficult to distinguish between tumor response and irradiated liver damage.

We recommend the following criteria for the evaluation of tumor response after SBRT with TACE based on dynamic CT appearance: (i) no tumor enlargement; (ii) continuous dense lipiodol accumulation; and (iii) disappearance of early arterial enhancement for a minimum of 6 months. However, tumors showing continuous residual early arterial enhancement should be followed up and reassessed at 12 months if no tumor enlargement is noted.

The dynamic CT scans used to study the effects of SBRT with TACE for HCC tumors had 4 patterns of response. Residual early arterial enhancement of a tumor observed 3 months after SBRT should not be considered a sign of tumor recurrence unless it persists until 6 months. Early assessment within 3 months may result in a misleading response evaluation.

Because of its retrospective nature, we are aware that this study has certain limitations, such as the low number of patients, extremely short follow-up periods,

no pathological findings for the described types of CT appearances and the effects of previous treatment. SBRT can still be considered an alternative to surgery, ablation and TACE when these therapies fail, and most of our patients had undergone those therapies previously, which possibly influenced the CT appearance of tumor responses after SBRT. We are currently planning a prospective study to address the points mentioned above.

REFERENCES

1 NCCN Clinical Practice Guidelines in Oncology (NCCN Guidelines). Hepatobiliary Cancers ver. 2. [home page on the internet]. Fort Washington, PA: National Comprehensive Cancer Network; [updated 2012 Jan 1]. Available at: http://www.nccn.org/professionals/physician_gls/f_guidelines.asp. Accessed March 12 2012

2 Thomas MB, Jaffe D, Choti MM *et al.* Hepatocellular carcinoma: consensus recommendations of the national cancer institute clinical trials planning meeting. *J Clin Oncol* 2010; **28**: 3994–4005.

3 Choi E, Rogers E, Ahmad S *et al.* Hepatobiliary cancers. In: Feig BW, Berger DH, Fuhrman GM, eds. *The M. D. Anderson Surgical Oncology Handbook*. Philadelphia, PA: Lippincott Williams &Wilkins, 2006; 320–66.

4 Andolino DL, Johnson CS, Maluccio M *et al.* Stereotactic body radiotherapy for primary hepatocellular carcinoma. *Int J Radiat Oncol Biol Phys* 2011; **81**: e447–e453.

5 Takeda A, Takahashi M, Kunieda E *et al.* Hypofractionated stereotactic radiotherapy with and without transarterial chemoembolization for small hepatocellular carcinoma not eligible for other ablation therapies: preliminary results for efficacy and toxicity. *Hepatol Res* 2008; **38**: 60–9.

6 Fukumitsu N, Sugahara S, Nakayama H *et al.* A prospective study of hypofractionated proton beam therapy for patients with hepatocellular carcinoma. *Int J Radiat Oncol Biol Phys* 2009; **74**: 831–6.

7 Kato H, Tsujii H, Miyamoto T *et al.* Results of the first prospective study of carbon ion radiotherapy for hepatocellular carcinoma with liver cirrhosis. *Int J Radiat Oncol Biol Phys* 2004; **59**: 1468–76.

8 Dawson LA. Overview: where does radiation therapy fit in the spectrum of liver cancer local – regional therapies? *Semin Radiat Oncol* 2011; **21**: 241–6.

9 Elsenhauer EA, Therasse P, Bogaerts J *et al.* New response evaluation criteria in solid tumors: revised RECIST guideline (version1.1). *Eur J Cancer* 2009; **45**: 228–47.

10 WHO. *WHO Handbook for Reporting Results of Cancer Treatment, Vol.* 48, Geneva: World Health Organization Offset Publication, 1979.

11 Kimura T, Hirokawa Y, Murakami Y *et al.* Reproducibility of organ position using voluntary breath-hold with spirometer for extracranial stereotactic radiotherapy. *Int J Radiat Oncol Biol Phys* 2004; **60**: 1307–13.

12 Kudo M, Kubo S, Takayasu K *et al.* Response Evaluation Criteria in Cancer of the Liver (RECICL) proposed by the Liver Cancer Study Group of Japan (2009 Revised Version). *Hepatol Res* 2010; **40**: 686–92.

13 Wulf J, Herfarth KK. Normal tissue dose constraints in stereotactic body radiation therapy for liver tumors. Stereotactic Body Radiation Therapy. In: Kavanagh BD, Timmerman RD, eds. *Stereotactic Body Radiation Therapy*. Philadelphia: Lippincott Williams & Wilkins, 2005; 39–45.

14 Sanuki-Fujimoto N, Takeda A, Ohashi T *et al.* CT evaluations of focal liver reactions following stereotactic body radiotherapy for small hepatocellular carcinoma with cirrhosis: relationship between imaging appearance and baseline liver function. *Br J Radiol* 2010; **83**: 1063–71.

15 Olsen CC, Welsh J, Kavanagh BD *et al.* Microscopic and macroscopic tumor and parenchymal effects of liver stereotactic body radiotherapy. *Int J Radiat Oncol Biol Phys* 2009; **73**: 1414–24.

16 Willemart S, Nicaise N, Struyven J, Van Gansbeke D. Acute radiation-induced hepatic injury: evaluation by triphasic contrast enhanced helical CT. *BJR* 2000; **73**: 544–6.

17 Takayasu K, Arii S, Matsuo N *et al.* Comparison of CT findings with resected specimens after chemoembolization with iodized oil for hepatocellular carcinoma. *AJR Am J Roentgenol* 2000; **175**: 699–704.